Modelling Small Electric Brushless Motors and Propellers

Please select category below:
Normal Paper ☒
Student Paper ☐
Young Engineer Paper ☐

Matthew Anderson[1,2], KC Wong[1] and Patrick Hendrick[2]
[1] *The University of Sydney, Sydney, NSW, Australia*
[2] *Universite Libre de Bruxelles, Brussels, Belgium*

Abstract

Propeller dynamics play an important role in the stability and controllability of multirotor unmanned aerial vehicles (UAVs), however are often greatly simplified or even neglected altogether when designing multirotor simulations. This paper presents a method for calculating and simulating the dynamics of a brushless motor and propeller typical of the size used in small multirotors so that the rotation speed and generated forces may be accurately reconstructed from an input pulse width modulation (PWM) signal.

The system model is identified using a series of sine-sweep inputs. Results show that the force and torque generated by the propeller and the power required can be accurately modelled from a raw input PWM signal, even for the dynamic case where the propeller is changing speed.

Keywords: Electric BLDC motor, motor modelling, ESC modelling.

Introduction

The problem of incorrectly modelled rotor dynamics is only made worse as multirotors are inherently unstable platforms. The flight controller must constantly vary each of the propeller speed commands, and large command changes can mean large variations between commanded rotation speed and the actual rotation speed, adversely affecting stability. While well designed control laws are often robust to unknown system dynamics, higher performance can be achieved by fully understanding the dynamics of the system being controlled (eg. rotational inertia of the propellers, and electronic speed controller (ESC)), which is not possible if the dynamics of the actuator are unknown[2].

Little work has been done on the unsteady modelling of small propellers and brushless motors. In simulation, propeller dynamics are often modelled using 1st order systems (for rotation speed) with steady force and torque data mapped to the RPM[2,3]. The time constants for the 1st order system are generally not given, leading to tests having to be repeated by each researcher. Khan et al [4] provide a very good model for estimating the propeller performance from specifications, including transient responses, though it has trouble matching the experimental data due to its method of implementation and shows only limited results. Interestingly, they also provide one of only a few methods that work from a PWM signal instead of a commanded RPM. This is an important addition as flight controllers generally are onle able to send PWM signals to the ESC to provide open-loop control of the motor speed.

System Model

The model for the system investigated in this paper is shown in Figure 1. Typically, papers which focus on multirotor control [3] assume that the RPM of the motor is known and can be controlled directly. In reality, most flight controllers (such as those based on the ArduPilot project) control the PWM signal sent to the ESC and the system operates open-loop from

there [5]. As such, it is important to be able to model how the PWM signal converts into propeller rotation and subsequently into the forces and torques provided to the vehicle to be able to tune these controllers off-line.

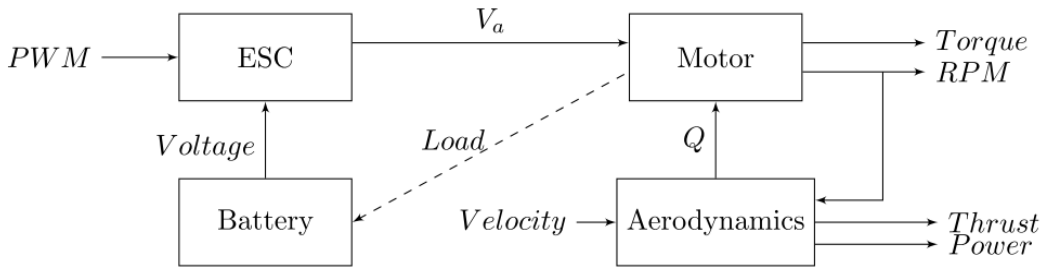

Fig. 1: The System Model

The input signal to the system is the PWM generated by the flight controller which is then (in the simplified case) converted into an armature voltage by the ESC using the voltage supplied by the battery. This armature voltage is fed into the motor which generates an RPM and torque and feeds a load back into the battery which in turn affects the battery voltage. This RPM generates the aerodynamic loads of thrust and aerodynamic torque. The aerodynamic torque feeds back into the motor and in turn affects the RPM and torque produced.

This paper models the ESC, motor and aerodynamic effects. As power is supplied from a bench power supply, the battery is not modelled, however the voltage and current supplied is directly measured and accounted for. Models for the battery can be found in other papers such as [4] and are easily integrated as a modifier to the supply voltage.

Experimental Setup

Hardware

The forces and torques produced by the propeller were measured using an ATI Nano25 load cell, logged on a NI-DAQ data acquisition box. The PWM signal is generated by an Arduino Pro Mini microprocessor at 200 Hz in order to reduce the effect of any on-board input averaging done by the ESC. The RPM is measured by the microprocessor using a custom optical sensor and the external interrupt pin in order to accurately time the period of revolution for the motor. The measured RPM and PWM signal are converted to an analogue signal by a digital to analogue converter and are fed into the NI-DAQ data acquisition box.

The supply voltage and current were measured using a custom power board. The phase voltage, used to calculate the armature voltage (or line voltage), was measured between ground and one of the three phase wires and is filtered using an RC filter with a cut-off frequency of 50 Hz. All the data channels were logged using a NI-DAQ logging at 2000 Hz interfaced through MATLAB.

The two motors tested were the Turnigy 1811-2900kV Electric Brushless and the Turnigy 2211-2300kV Electric Brushless, both of which were controlled by a Turnigy 10A Plush ESC using a supply voltage of approximately 8 V (around the voltage of a near-full 2S Lithium-Polymer battery). Five propellers were tested – a GWS Style 4x2.5, a GWS 4x4, a TGS Sport Electric 4.5x4.5, a GWS Style 5x3, and a GWS Style 6x3 where the propellers are defined by (diameter x geometric pitch) in inches.

Data Acquisition and Filtering

MATLAB was used to log and post-process the data collected from a NI-DAQ data acquisition box. The propeller and motor combination were dynamically balanced using the FFT of the force data to reduce the noise as much as possible. In order to help attenuate the high-frequency noise, foam was used to isolate the motor from the load cell. The data was digitally filtered using a frequency domain filter from [6] at a cut-off frequency of 30 Hz.

Steady-State System Identification

Steady-state system identification is much easier and requires less sophisticated equipment to generate results than dynamic system identification; therefore, properties are preferentially calculated using steady-state relationships. The results presented in this section are typical of what is generated thus only the results for the 1811-2900kV motor and 5x3 propeller are shown. The data was obtained from 10 different PWM sweeps of 21 data points between PWM lengths of 1100 and 1800 μs.

The static equations for thrust, torque and power are

$$T = C_T \cdot \rho\, D^4\, n^2 \quad (1)$$

$$Q = C_Q \cdot \rho\, D^5\, n^2 \quad (2)$$

$$P = C_P \cdot \rho\, D^5\, n^3 + c_{Watts} \quad (3)$$

where T is the thrust, C_T is the coefficient of thrust, ρ is the air density, D is the propeller diameter, n is the propeller rotation speed in revolutions per second, Q is the aerodynamic torque, C_Q is the coefficient of torque, P is the power, C_P is the coefficient of power and c_{Watts} is the baseline power required to run the system [7,8]. The results of the fit are shown in Figure 2 with ten sets of data shown to demonstrate the repeatability of the tests.

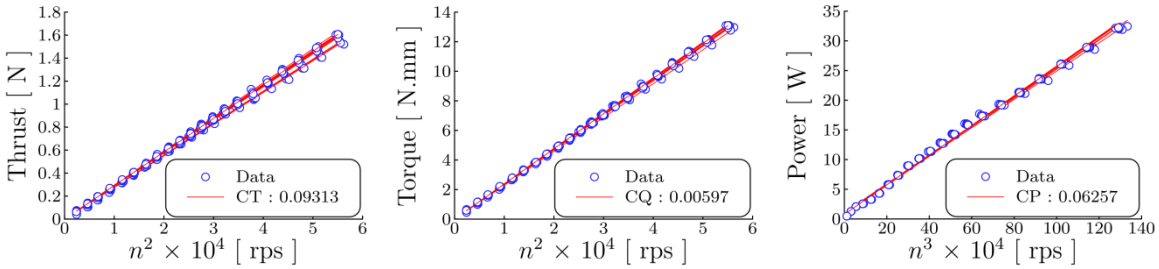

Fig. 2: Static fits for the GWS Style 5x3 and Turnigy 1811-2900kV Motor.

As to be expected, the static equations describe the thrust, torque and power well. C_T is estimated to be 0.0931, a value to be expected of a 5x3 (14.3 deg pitch) propeller [7]. Similarly, the torque and power fits match well to the experimental data, giving a C_Q of 0.0060, a C_P of 0.063 and a c_{Watts} of 0.86 W.

Armature Voltage (ESC Model)

The ESC controls the motor by generating a three-phase signal to pulse the poles of the motor and cause rotation. The "average voltage" of this signal is regulated by switching the voltage supply on and off very quickly within this three-phase signal. Higher-end ESCs control motors to a constant rotational speed, however typical hobbyist ESCs just regulate the power supplied and merely keep the three-phase field in time with the rotation of the motor. The functionality of the ESC has been simplified for the standard motor model so that the ESC provides an armature voltage for a given PWM signal.

The measured quantity was the phase voltage, taken between one of the three phase wires and ground just before the ESC. Due to the inverting nature of the MOFSETs in the ESC, the actual phase voltage was calculated by

$$V_{Phase_{Actual}} = V_{Battery} - V_{Phase_{Measured}} \tag{4}$$

This was converted into the line voltage by multiplying by a factor of $\sqrt{3}$ [4].

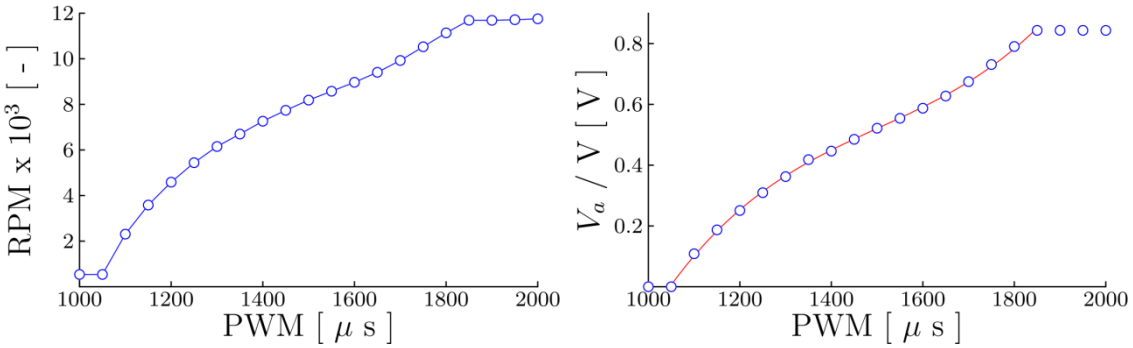

Fig. 3: PWM to RPM and Static V_{Line} / $V_{Battery}$ Fit

Figure 3 shows the static results for the measurement of V_{Line} / $V_{Battery}$. Testing showed that this function did not change with changing battery voltage; however it did change depending upon the motor and propeller combination. The reason for this change is unknown, however it is theorised that it has to do with the way the internal controllers of the ESC are designed to try and provide a linear thrust response with input PWM signal. The function of PWM to V_{Line} / $V_{Battery}$ was well described by a third-order polynomial.

Dynamic System Identification

Two systems identification methods were used to regress the dynamic data - linear regression for the thrust, torque and power and output-error estimation for the motor dynamics. As certain data could not be directly measured (such as the rate of change of the RPM), this data was obtained from other states (in this case, by differentiating the RPM) prior to filtering being conducted [6].

The dynamic test data was obtained from logarithmic sine-sweeps between 0 and 25 Hz. These sweeps were conducted at various different trim and PWM amplitudes to identify any non-linearities or inconsistent behaviours within the motors. Unsteady aerodynamic effects were ignored as these do not have a significant impact on propeller performance, even during very aggressive multirotor manoeuvres [1].

Dynamic Thrust, Torque and Power Identification

The equations for thrust, torque and power in the dynamic case are

$$T = C_T \cdot \rho\, D^4\, n^2 \tag{5}$$

$$\tau = J\dot{\omega} + K_d\omega + Q \tag{6}$$

$$P = C_P \times D^5 n^3 \rho + c_{Watts} + J\,\eta\,\dot{\omega} \tag{7}$$

where J is the inertia of all the rotating components (including the motor bell), ω is the rotational speed in rad/s, K_d is the damping constant between the motor stator and rotor, Q is the aerodynamic torque and η is the efficiency at which the ESC can accelerate the motor [4]. As with other work, K_d is assumed small and is not modelled [4].

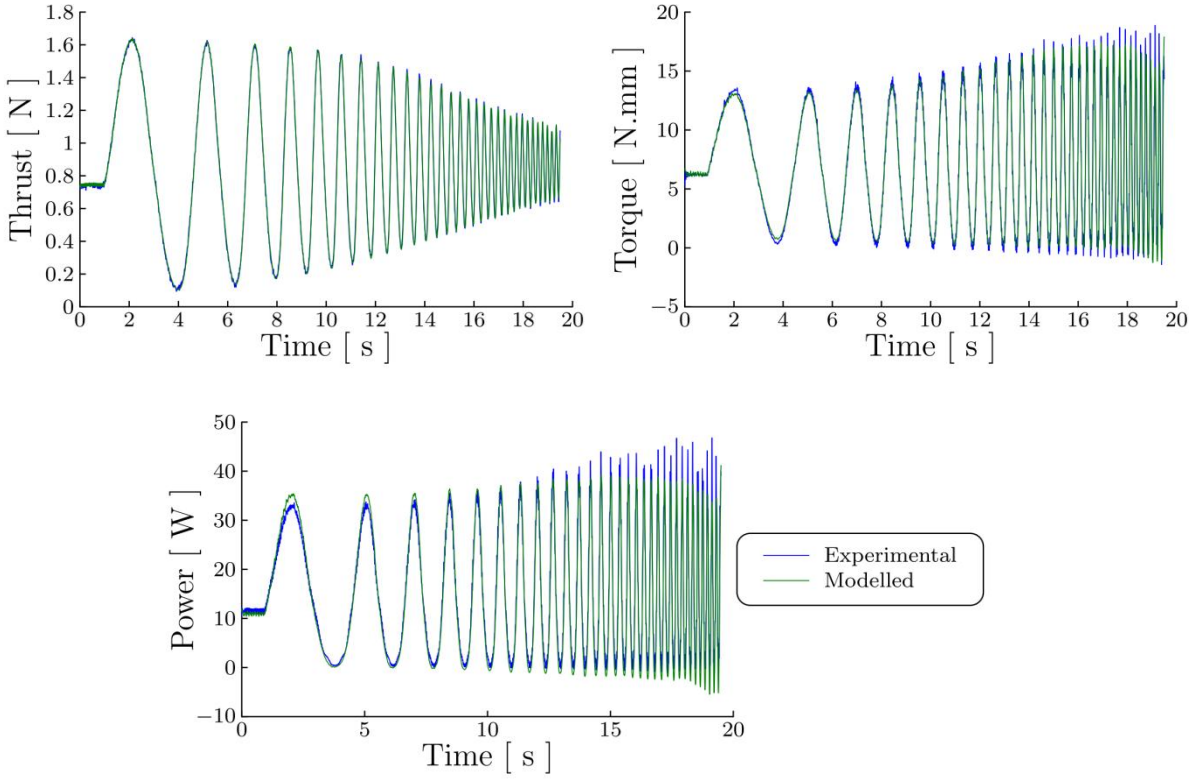

Fig. 4: Static Fits for the GWS Style 5x3 and Turnigy 1811-2900kV Motor.

The results of a typical dynamic fit in Figure 4 show very good correlation between the measured and fitted data, matching the peak amplitudes and frequencies well. The fits for the torque and power have some noise due to the experimental $\dot{\omega}$ term being noisy, however as can be seen, the peaks in torque and power due to RPM changes still match very well.

First Order Transfer Function Model

MATLAB was used to identify a first order model for the PWM to RPM signal, similar to those models used in [2,3]. The system, as identified at a trim PWM of 1500 μs with amplitudes of 50, 100, 200 and 300 μs,gave the similar identified model, averaging to

$$G(s) = \frac{112}{s + 11} \tag{8}$$

For small PWM changes around the trim value, the identified model works well as the change in RPM is approximately proportional to the change in PWM. For larger changes, this relation no longer holds valid (Figure 5), and though the frequency still matches, the amplitudes no longer match well. The bandwidth of the system is about 1.75 Hz.

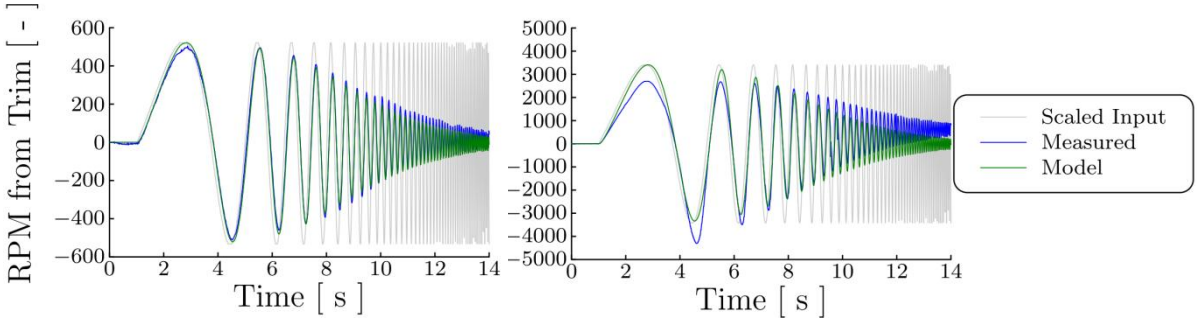

Fig. 5: Transfer Function Model Responses for Sweep Amplitudes of 50 and 300 μs

State Space Motor Model

A state-space model was generated as it is simpler to implement into a MATLAB-based, time-stepped simulation. The model is defined such that [4]

$$\begin{bmatrix} \dot{I}_a \\ \dot{\omega} \end{bmatrix} = \begin{bmatrix} -\frac{R_a}{L_a} & -\frac{K_v}{L_a} \\ \frac{K_v}{J} & -\frac{K_d}{J} \end{bmatrix} \begin{bmatrix} I_a \\ \omega \end{bmatrix} + \begin{bmatrix} \frac{1}{L_a} & 0 \\ 0 & -\frac{1}{J} \end{bmatrix} \begin{bmatrix} V_a \\ Q \end{bmatrix} \tag{9}$$

$$\begin{bmatrix} I_a \\ \omega \end{bmatrix} = \begin{bmatrix} 1 & 0 \\ 0 & 1 \end{bmatrix} \begin{bmatrix} I_a \\ \omega \end{bmatrix} + \begin{bmatrix} 0 & 0 \\ 0 & 0 \end{bmatrix} \begin{bmatrix} V_a \\ Q \end{bmatrix}$$

where R_a is the armature resistance, L_a is the inductance of the armature, K_v is the velocity constant, J is the polar moment of inertia of the rotating components and K_d is the damping between the rotor and the stator. The state variables are I_a, the armature current and ω, the angular rotational rate. The input variables are V_a, the armature voltage and the aerodynamic torque loading Q. K_d is once again assumed to be negligible. Given I_a is not measured, the system was trimmed to find the initial conditions with an input armature voltage and RPM using the Newton-Rhapson method.

Figure 6 shows a typical response for the rotational response for a given armature voltage input. The frequency is reproduced very well despite the amplitudes not matching so well.

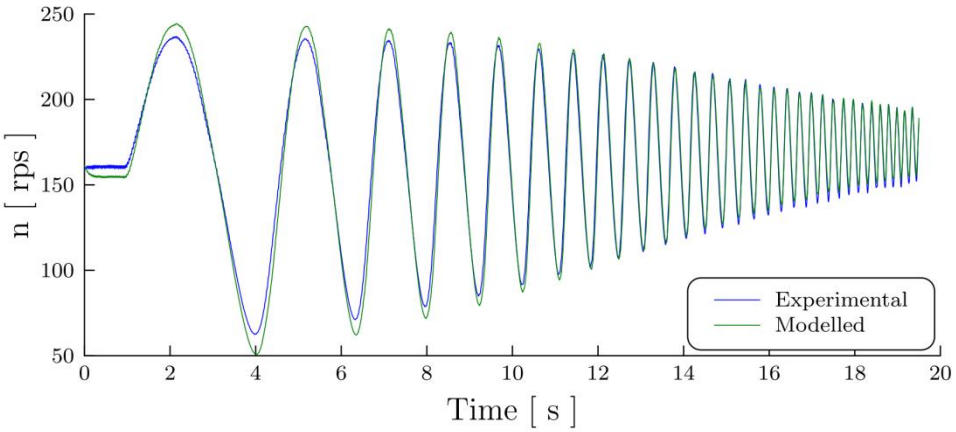

Fig. 6: Rotational Speed Fit for the GWS Style 5x3 and Turnigy 1811-2900kV Motor.

Multiple Motor / Propeller Combination Results

The following figures show the results for all the propeller/motor combinations as identified using dynamic data. Where possible, values identified in static testing were compared against those identified in dynamic testing and were found to match very well, within around ± 5 %.

Figure 7 shows the results of the parameters C_T, C_Q, C_P and c_{Watts}. The C_T and C_Q of the propellers estimated is near identical for both motors, and were very close to the values estimated in the static case. The C_P for the 2211-2300kV motor is lower than that for the 1811-2900kV motor, and exhibits a near constant offset. Though the average estimated C_P value matched the static estimated value, there was some spread in the dynamic estimates for C_P. Lundstrom, Amadori and Krus [9] found that ESC efficiency can vary between 30 and 70 % between low and high settings, and this most likely contributed to the data spread.

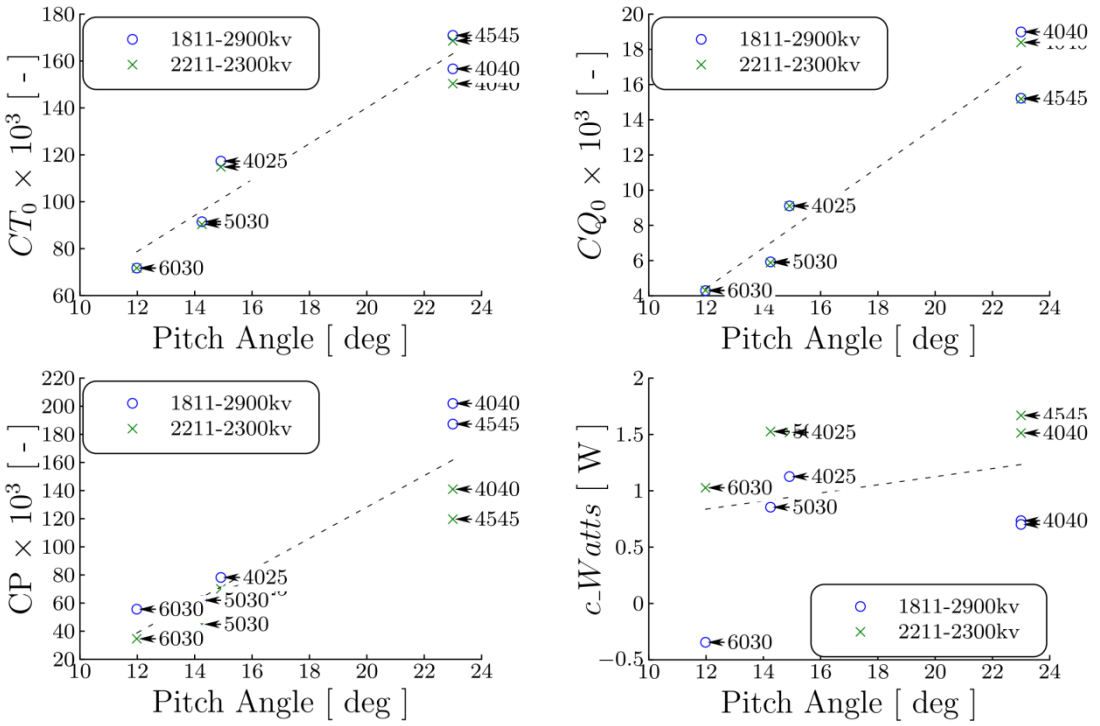

Fig. 7: Summary of Propeller Aerodynamic Estimate Data from Steady-State Testing.

Comparing the modelled power required to generate a given thrust (Figure 8) shows that the 2211-2300kV motor is far more efficient, requiring less power for every propeller except the 4x2.5 which represents an under-propped case. c_{Watts} is negative for the 1911-2900kV case as it is over-propped. Larger propellers produced more thrust with the same power.

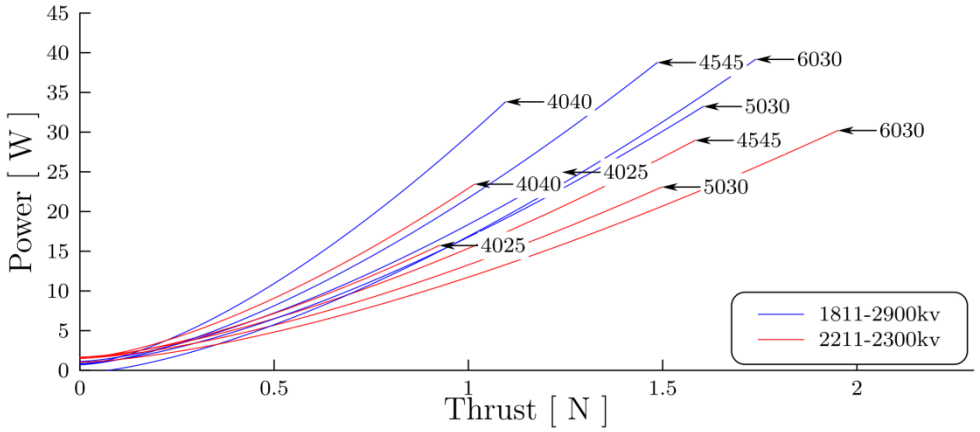

Fig. 8: Power Required for a Given Thrust for Each Motor and Propeller Combination

Figure 9 shows the estimated motor parameters. The predicted K_v for the 1811-2900kV motor of 2970 RPM/V matches very well to the manufacturer's K_v of 2900 RPM/V. For the 2211-2300kV, the match is not as good, estimating 1833 RPM/V for a 2300 RPM/V motor. L_a was estimated to be 3.8 x 10^{-4} H for the 1811-2900kV motor and 4.4 x 10^{-4} H for the 2211-2300kV motor.

The armature resistance of the 1811-2900kV is estimated to be significantly higher than of the 2211-2300kV which accounts for the significantly higher power requirement. The high standard deviation in the armature resistance estimate is potentially caused by constants not actually being constant due to secondary effects within the motor such as temperature [9].

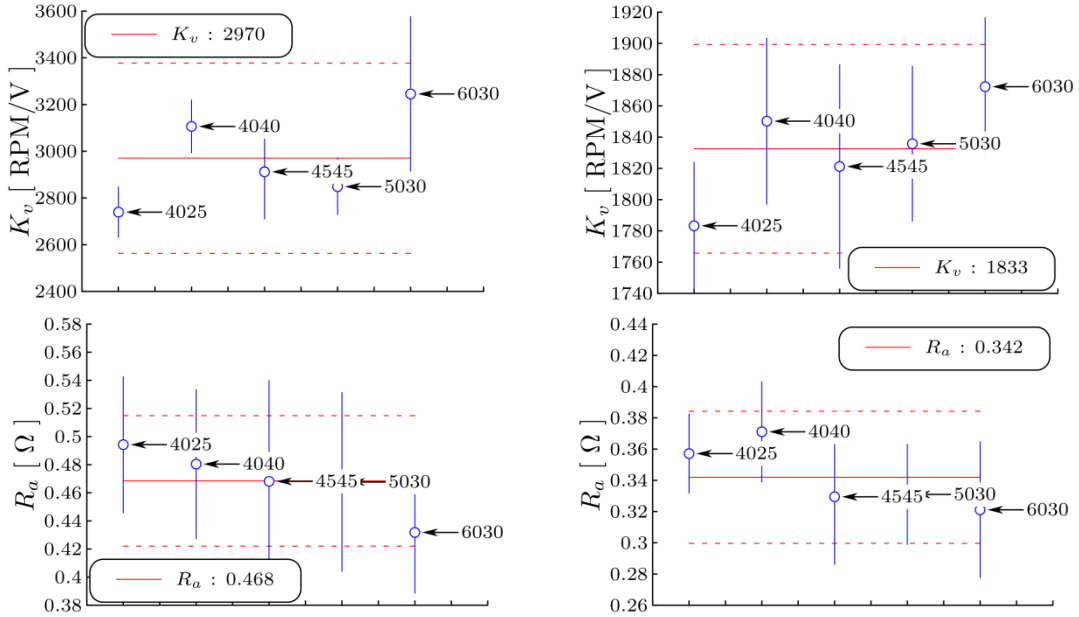

Fig. 9: Summary of Motor Data (Left: Turnigy 1811-2900kv, Right: Turning 2211-2300kv)

Figure 10 shows the estimates for the rotational inertia of all the motor and propeller combinations. The constant offset between each of the propeller pairs is the difference in inertia of the motor bells. The TGS 4.5x4.5 propeller has a larger inertia than the larger GWS Style 5x3 as the propeller is much more solid propeller and has a significantly larger mass. A SolidWorks model of the 5x3 propeller and 1811-2900kV motor predicts a J of 1670 kg.mm^3, a very good match to the dynamically estimated value of 1759 kg.mm^3.

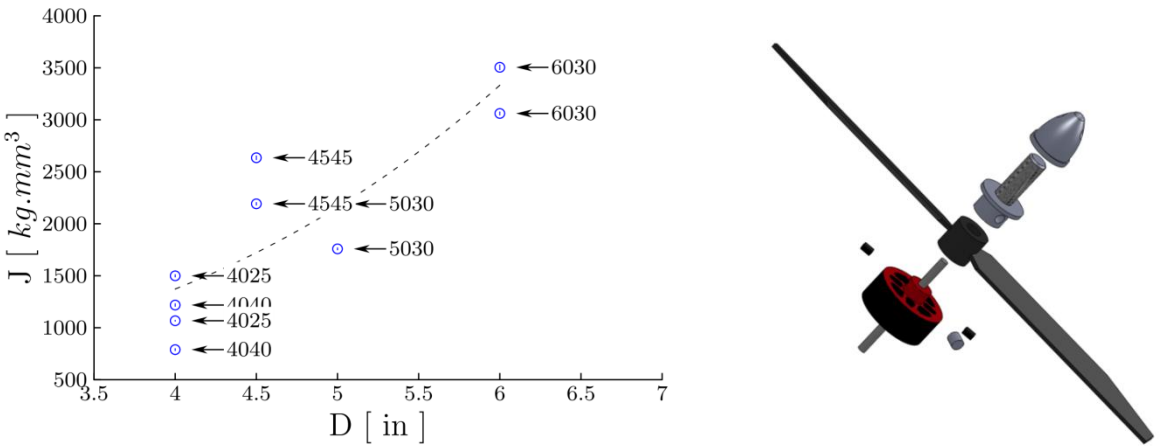

Fig. 10: Summary of Inertia Data for All Propellers and Motors and the SolidWorks Model

Verification

A series of step inputs were generated as a verification case for the system modelling. The coefficients used in the simulation were taken from the steady-state identification where possible and the motor data from the averaged motor parameters across all propellers. For the thrust, torque and power case, the RPM was predicted using the armature voltage, rather than using the measured RPM.

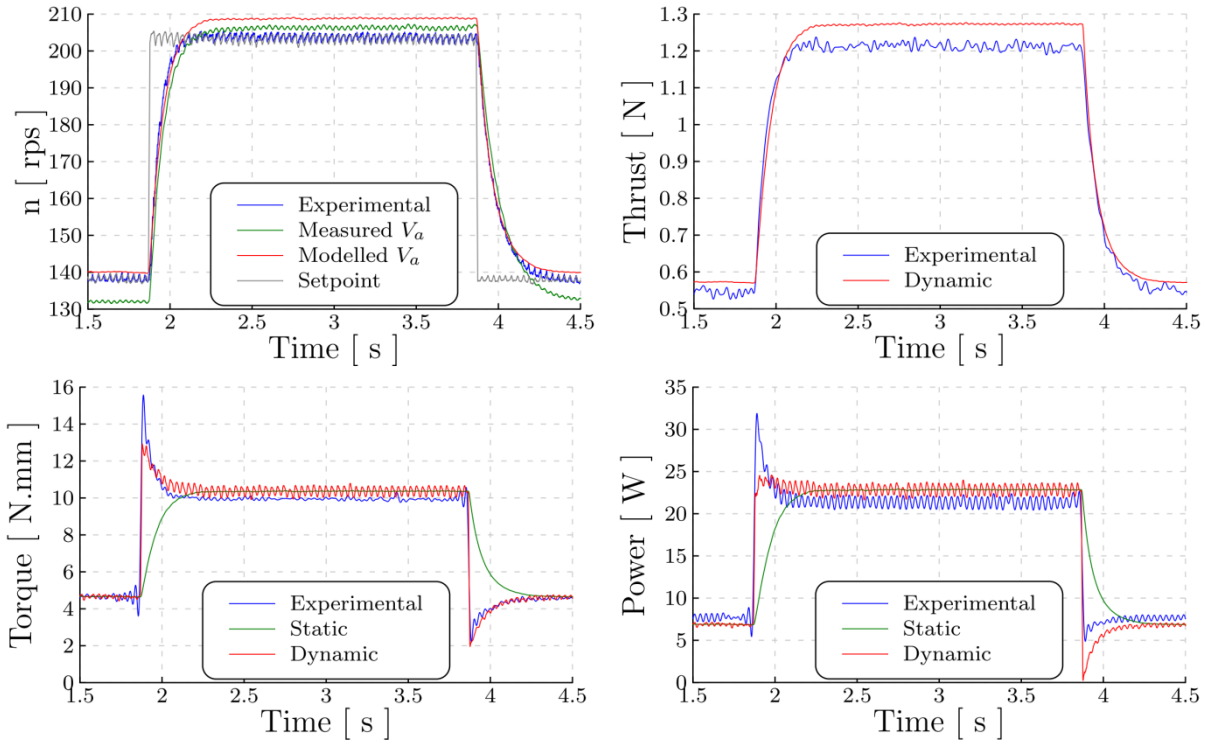

Fig. 11: Simulated Thrust Generated by the Propeller

The RPM response of the motor (Figure 11) was modelled using both the armature voltage as measured during the test and the armature voltage modelled from the input PWM signal. Interestingly, the simulated response using the modelled V_a is closer to the experimental data, though both simulated responses fall within about 7 % of the measured RPM. More importantly however, the rise time and dynamic behaviour of the motor is reproduced well. As with the RPM prediction, the thrust prediction mimics the dynamics well, though it does settle slightly higher than the experimental data. The experimental torque and power are shown along with two estimates - one utilising only the static terms and the other modelling the full dynamics. This shows the importance of modelling the dynamic terms as the motor experiences a very large 'kick' in torque when accelerating and de-accelerating the motor, a significant, but un-modelled feature in the static case.

As with the torque, the dynamic terms for power are very important and dominate the transient response. This can be important to model, especially if the batteries used suffer significant voltage sag under load as the transient power requirements can be much higher the in the steady case. The step-up doesn't peak as high as would be expected and the step-down greatly underestimates the required power. This results from the identification process trying to balance out differing the rising and falling characteristics of the power, stemming from the inability of the ESC model to replicate the 'catching' of the motor as it slow down.

Conclusion

This paper has presented a method for calculating the parameters for generating a dynamic model for a brushless motor using experimental data. Models for the ESC, propeller and motor were all developed and shown to predict the dynamic behaviour of the propeller RPM, thrust, torque and power consumption well. This enables systems that are heavily reliant on thrusters (such as multirotors) to be accurately modelled so that accurate multirotor simulations can be built.

References

1. Pounds, P.; Mahoney, R. & Corke, P., Design of a Static Thruster for Microair Vehicle Rotorcraft, *Journal of Aerospace Engineering*, 2009, *22*, 85-94.

2. Pounds, P., Mahoney, R., Gresham, J., Corke, P. & Roberts, J., Towards Dynamically-Favourable Quad-Rotor Aerial Robots, *Australasian Conference on Robotics and Automation (ACRA 2004)*, Canberra, 2004.

3. Bangura, M. & Mahony, R., Nonlinear Dynamic Modeling for High Performance Control of a Quadrotor, *Australasian Conference on Robotics and Automation*, 2012.

4. Khan, W. & Nahon, M., Toward and Accurate Physics-Based UAV Thruster Model, *Transactions on Mechatronics*, 2013, *18*, 1269-1279.

5. ArduPilot.org, APM:Copter Documentation, http://ardupilot.org/. Accessed Dec. ’16.

6. Klein, V. & Morelli, E., Aircraft System Identification: Theory and Practice, *AIAA*, 2006.

7. Gray, W. , Wind-Tunnel Tests of Single- and Dual-Rotating Tractor Propellers at Low Blade Angles and of Two- and Three Blade Tractor Propellers at Blade Angles up to 65 deg, *Langley Memorial Aeronautical Laboratory, NACA*, 1943.

8. Brandt, J. & Selig, M., “Propeller Performance Data at Low Reynolds Numbers”, *49th AIAA Aerospace Sciences Meeting*, 4-7 January 2011, Orlando.

9. Lundström, D., Amadori, K. & Krus, P, “Validation of Models for Small Scale Electric Propulsion Systems”s, *48th AIAA Aerospace Sciences Meeting Including the New Horizons Forum and Aerospace Exposition*, 2010.